Capture of low-energy electrons by simple closed-shell metal clusters

P.-A. Hervieux,[1] M. E. Madjet,[2] and H. Benali[1]

[1]*Laboratoire de Physique Moléculaire et des Collisions, Institut de Physique, 1 Rue Arago, Technopôle 2000,*
Université de Metz, 57078 Metz Cedex 03, France
[2]*Max-Planck-Institut für Physik Komplexer Systeme, Nöthnitzer Strasse 38, D-01187 Dresden, Germany*

The capture by polarization forces of low-energy electrons by closed-shell sodium clusters has been studied in the framework of the time-dependent local density approximation within the spherical jellium model and the classical scattering theory of Langevin. Results for Na_{20}, Na_{40}, and Na_{58} are compared with the predictions of the classical image charge model and recent experimental results by Kasperovich *et al.* [Phys. Rev. A **60**, 3071 (1999)].

I. INTRODUCTION

Atomic clusters constitute a bridge between atomic, molecular, surface, and condensed matter physics. Among all the types of clusters, metal clusters, and in particular alkali metal clusters, have been intensively investigated experimentally and theoretically in order to have a better comprehension of the evolution of electronic size effects [1,2]. At present, mass selected free metal clusters are experimentally available, which clears the way for a clean and meaningful study of their interactions with all kinds of projectiles including light (e.g., photons [3], electrons [4]) and heavy particles (e.g., atoms [5], molecules, surfaces). In particular, inelastic scattering of low-energy electrons on metallic clusters is a process of fundamental interest since it provides a very powerful way for studying many-electron correlations in quantum finite systems [6].

Since metal clusters are highly polarizable objects, it is well known that, in the case of the scattering of slow electrons by neutral metal clusters, the first important force affecting the incoming electron is the polarization of the cluster by the projectile field. At large distances this force is equivalent to the presence of a potential having the usual expression $-\alpha_{L=1}(\omega=0)/2r^4$ where $\alpha_{L=1}(\omega=0)$ is the static electric dipole polarizability of the cluster. This last quantity has been measured for selected sizes of sodium, potassium [7], and very recently lithium clusters [8]. Generally, in electron-atom or electron-molecule collisions, polarization effects may be properly included by taking into account only the dipole term of the full polarization potential. Until very recently, the same procedure was assumed to be valid in electron–metal-cluster collisions [9]. However, in a very recent paper devoted to the capture of low-energy electrons by large ($\sim 10^4$ atoms) free sodium clusters [10], Kasperovich *et al.* have shown that, in order to obtain good agreement with their experimental results, it is necessary to go beyond the dipole approximation. The model used in [10] to mimic the full static polarization potential is the classical image charge model describing the interaction of a point charge in front of a macroscopic neutral conducting sphere [11]. This classical approach is certainly valid for large clusters. For smaller sizes, one may doubt the validity of such a macroscopic approach. In the present work, we have evalu-

ated static multipolar polarization by using a microscopic theory based on the time-dependent local density approximation (TDLDA) and the spherical jellium model. In this way one can simulate from a purely microscopic many-body theory the static response of the valence electrons within the cluster to the electric field of the impacting electron.

As an application and due to the availability of experimental data, we have studied the capture of low-energy electrons by small closed-shell sodium clusters within the classical scattering theory of Langevin.

Our theoretical approach is outlined in the next section. Results concerning neutral closed-shell sodium clusters having 20, 40, and 58 valence electrons are given in Sec. III and compared with recent experimental results. Finally, we give a conclusion and discuss some perspectives of this work in Sec. IV. Atomic units are used unless otherwise specified.

II. THEORETICAL METHOD

A. Cluster description

The clusters are described in the spherical background jellium model, which is known to be a very good approximation for closed-shell simple metal clusters. This model consists in replacing the real ionic core potential by a constant positive background corresponding to a uniformly distributed charge density. For a metal cluster having A singly charged ionic cores, this potential is given by

$$V_{jel}(r) = \begin{cases} -\dfrac{A}{2R_C}\left[3-\left(\dfrac{r}{R_C}\right)^2\right] & \text{for} \quad r \leq R_C \\[2mm] -\dfrac{A}{r} & \text{for} \quad r > R_C, \end{cases} \quad (1)$$

where $R_C = A^{1/3}r_s$ and r_s is the Wigner-Seitz radius ($r_s=4$ for sodium clusters). In the Kohn-Sham formulation of density functional theory, the ground-state electronic density ρ_C of an N-electron system is written in terms of single-particle orbitals ϕ_i as

$$\rho_C(\vec{r}) = \sum_{i=1}^{N} \rho_i(\vec{r}) = \sum_i |\phi_i(\vec{r})|^2. \qquad (2)$$

These orbitals obey the Schrödinger equation

$$\left[-\frac{1}{2}\nabla^2 + V_{KS}(\vec{r}) \right] \phi_i(\vec{r}) = \epsilon_i \phi_i(\vec{r}), \qquad (3)$$

where $V_{KS}(\vec{r})$ is an effective single-particle potential given by

$$V_{KS}(\vec{r}) = V_{jel}(\vec{r}) + V_H(\rho_C(\vec{r})) + V_{xc}(\rho_C(\vec{r})), \qquad (4)$$

with $V_H(\rho_C(\vec{r}))$ the Hartree potential and $V_{xc}(\rho_C(\vec{r}))$ the exchange-correlation potential. Since the form of V_{xc} is not known in general, several approximations have been proposed in the literature. In this work, we have used the form obtained by Gunnarsson and Lundqvist [12] in the framework of the local density approximation:

$$V_{xc}(\rho_C(\vec{r})) = -\left(\frac{3\rho_C(\vec{r})}{\pi} \right)^{1/3} - 0.0333 \ln\left(1 + \frac{11.4}{r_s(\vec{r})} \right) \quad (5)$$

where $r_s(\vec{r}) = [3/4\pi\rho_C(\vec{r})]^{1/3}$ is the local Wigner-Seitz radius. The net charge of the cluster is $q_2 = A - N$.

B. Time-dependent local density approximation

If the system is in a weak external static field, the theory of the linear response (first order many-body theory) [13,14] relates the static induced electronic density $\delta\rho(\vec{r};[a])$ to the external potential $V_{ext}(\vec{r};[a])$ by the following relation:

$$\delta\rho(\vec{r};[a]) = \int \chi(\vec{r},\vec{r}') V_{ext}(\vec{r}';[a]) d\vec{r}' \qquad (6)$$

where $\chi(\vec{r},\vec{r}')$ is the static response function and $[a]$ represents a set of parameters. For the process considered here, V_{ext} is just the electrostatic interaction between the external particle of charge q_1 and the N valence electrons and is given by

$$V_{ext}(\vec{r};\vec{R}) = \sum_{j=1}^{N} \frac{-q_1}{|\vec{R} - \vec{r}_j|}, \qquad (7)$$

where $\vec{R}$ and $\vec{r}_j$ describe the positions of the external particle and valence electrons, respectively. For the sake of clarity, the set of vectors $\vec{r}_j$ will be represented by $\vec{r}$. It is possible to rewrite the static induced density given in Eq. (6) as

$$\delta\rho(\vec{r};\vec{R}) = \int \chi^0(\vec{r},\vec{r}')[V_{ext}(\vec{r}';\vec{R}) + V_{ind}(\vec{r}';\vec{R})]d\vec{r}'. \qquad (8)$$

In the above expression, χ^0 and $V_{ind}(\vec{r}';\vec{R})$ are, respectively, the noninteracting static response function and the induced potential (at position $\vec{r}'$) due to the polarization of the cluster
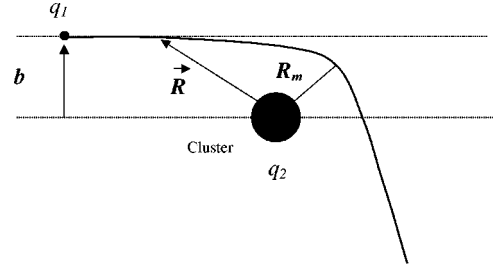

FIG. 1. Coordinates and notation used in the text.

electron cloud by the external particle (situated at position $\vec{R}$; see Fig. 1). V_{ind} can be written as

$$V_{ind}(\vec{r};\vec{R}) = \int \frac{\delta\rho(\vec{r}';\vec{R})}{|\vec{r} - \vec{r}'|} d\vec{r}' + \left[\frac{\partial V_{xc}}{\partial \rho} \right]_{\rho = \rho_C} \delta\rho(\vec{r};\vec{R})$$

$$= V_{ind}^C(\vec{r};\vec{R}) + V_{ind}^{xc}(\vec{r};\vec{R}), \qquad (9)$$

where ρ_C denotes the electronic density of the ground state calculated within the local density approximation and given in Eq. (2). Since we are concerned only with the interaction potential between the external charge q_1 and the cluster electronic distribution, one also defines the polarization interaction energy as

$$U_p(\vec{R}) = \frac{q_1}{2} \int \frac{\delta\rho(\vec{r}';\vec{R})}{|\vec{R} - \vec{r}'|} d\vec{r}' = \frac{q_1}{2} V_{ind}^C(\vec{R};\vec{R}). \qquad (10)$$

In the following, we shall use $V_{ind}^C(\vec{R})$ instead of $V_{ind}^C(\vec{R};\vec{R})$. For spherically symmetric systems (closed-shell metal clusters) the static response function χ may be written as

$$\chi(\vec{r},\vec{r}') = \sum_{L'M'} \frac{\chi_{L'}(r,r')}{(rr')^2} Y_{L'M'}^*(\hat{r}) Y_{L'M'}(\hat{r}') \qquad (11)$$

and, as usual, the Coulomb interaction is expanded as

$$\frac{1}{|\vec{R} - \vec{r}'|} = \sum_{LM} \frac{4\pi}{(2L+1)} \frac{r_<^L}{r_>^{L+1}} Y_{LM}^*(\hat{R}) Y_{LM}(\hat{r}'), \qquad (12)$$

with $r_< = \min(R,r')$ and $r_> = \max(R,r')$. Inserting the two preceding expressions into Eq. (6) leads to

$$\delta\rho(\vec{r};\vec{R}) = -q_1 \sum_{LM} \frac{\delta\rho_L(r;R)}{r^2} Y_{LM}^*(\hat{r}) Y_{LM}(\hat{R}) \qquad (13)$$

with the multipolar density of transition defined by

$$\delta\rho_L(r;R) = \frac{4\pi}{(2L+1)} \int_0^\infty \chi_L(r,r') \frac{r_<^L}{r_>^{L+1}} dr'. \qquad (14)$$

The static response function $\chi(\vec{r},\vec{r}')$ is a solution of the integral equation

$$\chi(\vec{r},\vec{r}')=\chi^0(\vec{r},\vec{r}')+\int\int\chi^0(\vec{r},\vec{r}'')$$
$$\times\left[\frac{\partial V_{KS}}{\partial\rho}\right]_{\rho=\rho_C}\chi(\vec{r}''',\vec{r}')d\vec{r}''d\vec{r}'''. \quad (15)$$

$\chi^0(\vec{r},\vec{r}')$ is the independent-particle static response function, which is given by

$$\chi^0(\vec{r},\vec{r}')=\sum_i^{occ}\phi_i^*(\vec{r})\phi_i(\vec{r}')G(\vec{r},\vec{r}';\epsilon_i)$$
$$+\phi_i(\vec{r})\phi_i^*(\vec{r}')G^*(\vec{r},\vec{r}';\epsilon_i)$$
$$=\sum_{\tilde{l}\tilde{m}}\frac{\chi_{\tilde{l}}^0(r,r')}{(rr')^2}Y_{\tilde{l}\tilde{m}}^*(\hat{r})\ Y_{\tilde{l}\tilde{m}}(\hat{r}') \quad (16)$$

where ϵ_i and $\phi_i(\vec{r})=(P_{nl}/r)rY_{lm}(\hat{r})$ are the eigenvalues and eigenfunctions of the Kohn-Sham equation (3) and $G(\vec{r},\vec{r}';E)$ is the retarded Green's function, which may be expanded as

$$G(\vec{r},\vec{r}';E)=\sum_{L'M'}\frac{G_{L'}(r,r';E)}{rr'}Y_{L'M'}^*(\hat{r})Y_{L'M'}(\hat{r}'). \quad (17)$$

It is easy to show that for the static case

$$\chi_L^0(r,r')=4\sum_{nlL'}P_{nl}(r)P_{nl}(r')\frac{(2l+1)(2L'+1)}{4\pi}$$
$$\times\begin{pmatrix}l & L' & L\\0 & 0 & 0\end{pmatrix}^2 G_{L'}(r,r';\epsilon_{nl}). \quad (18)$$

The radial part of the Green's function $G_l(r,r';E)$ may be expressed in terms of solutions of the radial homogeneous equation at energy $E=\frac{1}{2}k^2$:

$$\left[\frac{d^2}{dr^2}-\frac{l(l+1)}{r^2}-2V_{KS}(r)+k^2\right]\chi_l(r)=0. \quad (19)$$

Denoting by $w_l(r)$ the solution of Eq. (19) that behaves asymptotically as an outgoing wave and $u_l(r)$ the solution that is regular at the origin, we have

$$G_l(r,r';E)=\frac{u_l(r_<)w_l(r_>)}{W[u,w]} \quad (20)$$

where we have used $r_<=\min(r,r')$, $r_>=\max(r,r')$, and $W[u,w]$ is the Wronskian of the functions $u_l(r)$ and $w_l(r)$. Once the radial Green's functions are computed, $\chi^0(\vec{r},\vec{r}')$ may be constructed from Eq. (16), and the static response function $\chi(\vec{r},\vec{r}')$ is then obtained by solving the integral equation (15) with the use of a space discretization procedure.

Apart from simple poles at the bound state energies ϵ_{nl}, the Green's function $G_l(r,r';E)$ is analytic for complex values of the energy E. Due to the selection rules of the

Clebsch-Gordan coefficient in the expression (18), it turns out that, for even multipoles ($L=2k$ with $k\in\mathbf{N}$), the situation $L'=l$ and $E=\epsilon_{nl}(\omega=0)$ appears and the computation of G_l can no longer be carried out with the use of Eq. (20). In order to overcome this difficulty, we have employed the procedure of Stott *et al.* developed originally for closed-shell atoms and described in detail in Ref. [15]. It is worth noting that this problem does not occur either for the calculation of the dynamical response function ($\omega\neq0$) or for the calculation of the static dipole response ($\omega=0,L=1$).

By using the expressions (12), (13), and (14), one then may write U_p as

$$U_p(\vec{R})=U_p(R)=-\frac{q_1^2}{2}\sum_L\int_0^\infty\delta\rho_L(r,R)\frac{r_<^L}{r_>^{L+1}}dr. \quad (21)$$

It is easy to check the asymptotic behavior of U_p:

$$U_p(R)\sim-\frac{q_1^2}{2}\sum_{L=1}^\infty\frac{\alpha_L(0)}{R^{2L+2}}, \qquad R\to\infty, \quad (22)$$

where $\alpha_L(0)$ are the static multipolar polarizabilities given by

$$\alpha_L(\omega=0)=\frac{4\pi}{(2L+1)}\int_0^\infty\int_0^\infty\chi_L(r,r')(rr')^L dr\,dr'. \quad (23)$$

For the dipole contribution ($L=1$) and for neutral clusters ($q_2=0$), the leading term of the polarization interaction energy at large distances has the usual expression $-q_1^2\alpha_1(0)/2R^4$. One also notes that U_p does not depend on the sign of the projectile charge q_1. Thus, an electron ($q_1<0$) or a positron ($q_1>0$) will induce the same polarization energy.

In a pure classical macroscopic electrostatic model one may idealize a closed-shell simple metal cluster as being a conducting sphere of radius R_C with a sharp surface. Then, by using the image charge method, the interaction energy of a point charge in front of a neutral metallic sphere (i.e., $R>R_C$) can be obtained in a closed form and is given by [11]

$$U_p(R)\equiv U_p^M(R)=-\frac{q_1^2R_C^3}{2R^2(R^2-R_C^2)}, \quad (24)$$

with the multipolar expansion

$$U_p^M(R)=-\frac{q_1^2R_C^3}{2R^4}-\frac{q_1^2R_C^5}{2R^6}-\frac{q_1^2R_C^{2l+1}}{2R^{2l+2}}-\cdots. \quad (25)$$

Thus, from the above expression one sees that $\alpha_1^{cl}(0)\equiv R_C^3$ represents the classical static dipole polarizability and $\alpha_2^{cl}(0)\equiv R_C^5$ the quadrupole one.

The full interaction potential between the incoming particle of charge q_1 and energy E and a closed-shell metal cluster of charge q_2 is given by

$$U(R) = -q_1 V_{jel}(R) - q_1 \int \frac{\rho_C(\vec{r}')}{|\vec{R} - \vec{r}'|} d\vec{r}' + U_p(R) + U_x(R; E)$$

$$(26)$$

where the first term describes the interaction with the positive background and the second one the interaction with the ground-state electronic density (Hartree potential). Finally, U_x is present only when the projectile is an electron and is an energy-dependent potential representing the possibility for an incoming electron to be exchanged with one valence cluster electron [16]. For instance, this expression can be used to compute electron elastic cross sections [9]. Unfortunately, so far, no experimental data for this process are available.

As we shall see later, in the impact energy range considered in this work, $E < 3$ eV, and in a classical picture, the capture process occurs at distances well above the cluster radius. Thus, by noting that U_x is a short-range potential, the interaction potential relevant to our study takes the form [17]

$$U(R) = \frac{q_1 q_2}{R} + U_p(R). \tag{27}$$

C. Capture cross section

The scattering problem is treated classically in a way similar to that of the well-known Langevin theory of ion-molecule reaction [18,19]. Since experimental data are available for collisions of electrons impacting on neutral clusters, in the following, we shall restrict our study to $q_1 = -1$ and $q_2 = 0$. Futhermore, one knows from classical mechanics [20] that, in order to have trajectories approaching the cluster center (and leading to the capture of the projectile), the expansion of $U(R)$ in powers of R must include only terms R^{-n} with $n > 2$. This condition is not fulfilled for charged clusters due to the presence of the Coulomb interaction.

As pointed out by Kasperovich *et al.* [21] and demonstrated by Vogt and Wannier [22], in the impact energy range under consideration ($E < 3$ eV and not very low energy), the quantum capture cross section for a polarization potential $-q_1^2 \alpha_1(0)/2R^4$ is essentially equal to the classical one. Since this result is true for the singular potential above we do not know if it still remains valid for the full interaction potential, which is not singular at the origin (e.g., see Fig. 2). The answer to this question will be a matter of future work.

The procedure to obtain the classical capture cross section is given in Ref. [20] and is the following. For a given impact parameter b and an energy E, the effective potential is given by

$$U_{eff}(R, b) = \frac{b^2 E}{R^2} + U_p(R) \tag{28}$$

where $b^2 E / R^2$ is the centrifugal potential. Let $U_{eff}^m(b)$ be the maximum of the function $U_{eff}(R, b)$. The critical impact parameter b_0 (see below) is obtained from the condition $E = U_{eff}^m(b_0)$ and the corresponding capture cross section is given by
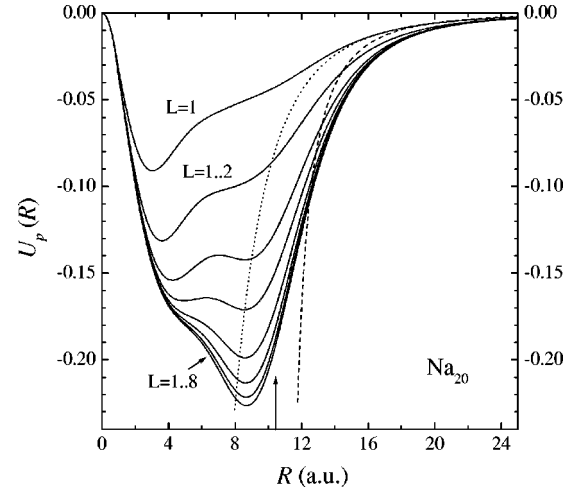

FIG. 2. Polarization interaction potential as a function of R for Na_{20}. Full line, U_p from Eq. (21) with $L = 1-8$; dashed line, U_p from Eq. (24); dotted line, $U_p = -q_1^2 \alpha_1(0)/2R^4$. The arrow at the bottom of the figure indicates the position of the cluster radius.

$$\sigma_{cap}(E) = \pi b_0^2. \tag{29}$$

One may understand the meaning of b_0 as follows. Classical orbits for which $b < b_0$ pass through the origin and therefore must lead to the capture reaction. On the contrary, capture does not occur for all collisions for which $b > b_0$.

For $U_p(R) = -\alpha_1(0)/2R^4$, the distance of closest approach associated with $b = b_0$ equals $R_{m0} = b_0/\sqrt{2}$ [19,22]. We have checked numerically (e.g. see Fig. 3) that, for the full interaction (26), $R_{m0} = b_0/a$ with $a < \sqrt{2}$. Thus, due to the fact that classically the details of $U(R)$ for $R < R_{m0}$ are not needed for the computation of the capture cross section and R_{m0} is always much larger than the cluster radius, this
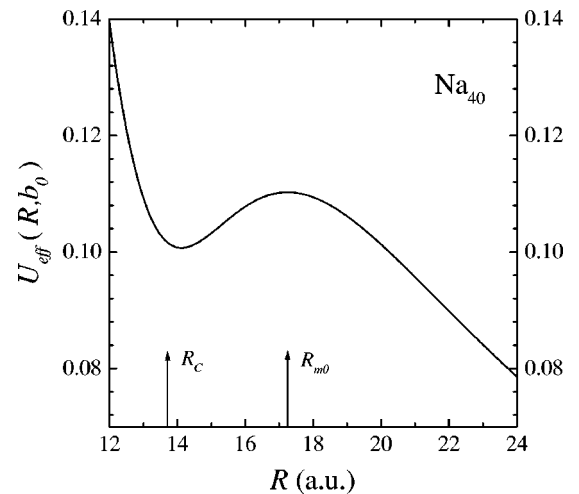

FIG. 3. Effective potential from Eq. (28) as a function of R for an electron of energy $E = 3$ eV impacting on Na_{40} and evaluated at $b = b_0 = 21.38$ a.u. The arrows at the bottom of the figure indicate the positions of the cluster surface and the distance of closest approach R_{m0}.

TABLE I. TDLDA static dipole and quadrupole polarizabilities normalized to the corresponding classical ones.

Cluster	$\alpha_1(0)/\alpha_1^{cl}(0)$	$\alpha_2(0)/\alpha_2^{cl}(0)$
Na_{20}	1.448	1.861
Na_{40}	1.412	1.654
Na_{58}	1.290	1.566

justifies the use of a first order many-body theory (TDLDA) and also the use in the calculation of Eq. (27) instead of Eq. (26).

If in Eq. (28) one uses $U_p(R) = -\alpha_1(0)/2R^4$ the result is analytical [20] and we obtain the so-called Langevin cross section

$$\sigma_{cap}(E) = \left[\frac{2\pi^2\alpha_1(0)}{E}\right]^{1/2}. \tag{30}$$

Futhermore, as shown by Klots [23] if in Eq. (28) $U_p(R) = U_p^M(R)$ the result is also analytical and reads

$$\sigma_{cap}(E) = \pi R_c^2 + \left[\frac{2\pi^2 R_c^3}{E}\right]^{1/2}. \tag{31}$$

For an interaction potential having an arbitrary shape the capture cross section must be computed using numerical methods.

III. RESULTS

So far, only static electric dipole polarizabilities have been measured for selected sizes of sodium, potassium [7], and lithium clusters [8]. As far as we know, theoretically as well as experimentally, nothing is known for metal clusters about static electric polarizabilities with $L \neq 1$. One may think that this lack is due to evident experimental and theoretical difficulties (see the evaluation of the Green's function in Sec. II B). This situation is in contrast with the atomic case for which theoretical and experimental data are available for quadrupole polarizabilities [15]. The TDLDA static dipole and quadrupole polarizabilities for Na_{20}, Na_{40}, and Na_{58} are given in Table I. For a given cluster size, the ratio $\alpha_L(0)/\alpha_L^{cl}(0)$ is larger for $L=2$ and decreases with increasing number of atoms.

Figure 2 shows the polarization interaction potential U_p as a function of R for Na_{20}. One sees that the convergence of the sum appearing in Eq. (21) is achieved for all distances with $L_{max}=8$. For $R > R_C$ the convergence is faster than in the interior region of the cluster and, for instance, for $R \geq 16$ a.u. the value of L_{max} is reduced to 4. Furthermore, the dipole contribution ($L_{max}=1$) reaches its asymptotic behavior around $R=16$ a.u., which is well outside the cluster radius $R_C=10.86$ a.u. One notes also that, unlike the commonly used polarization potential $-q_1^2\alpha_1(0)/2R^4$, U_p is not singular at the origin. For comparison, the macroscopic interaction given by the image charge model is also shown. For this small cluster size, the difference between the micro-
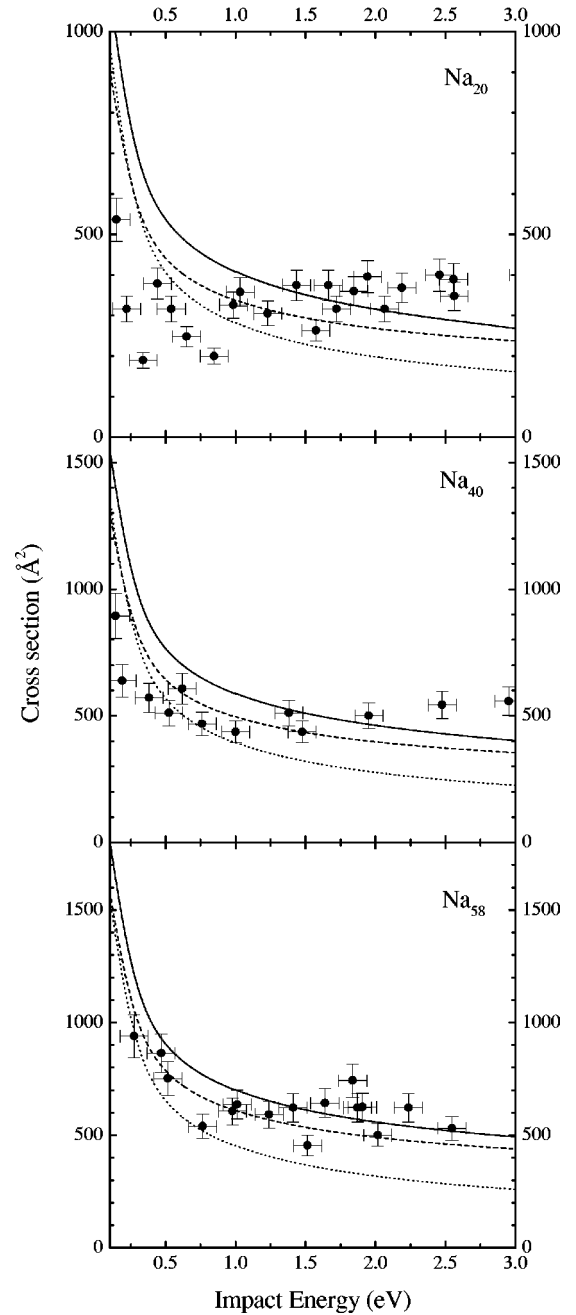

FIG. 4. Capture cross sections convoluted with the electron gun energy spread as functions of the electron impact energy E_i for three closed-shell sodium clusters. Full line, U_p from Eq. (21) with $L=1–8$; dashed line, U_p from Eq. (24); dotted line, $U_p = -q_1^2\alpha_1(0)/2R^4$; dots with error bars, experimental inelastic cross sections [24].

scopic (TDLDA) and the macroscopic results is rather important.

In order to illustrate the fact that, in a classical picture, the capture process occurs far away from the cluster surface, we show in Fig. 3 the effective potential obtained from Eq. (28) as a function of R for an electron energy of 3 eV impacting on Na_{40} and evaluated at $b=b_0=21.38$ a.u. This value is obtained as described in Sec. II C and the value 3 eV corresponds to the maximun electron energy considered in this

work. Since the distance of closest approach is much larger than $R_C = 13.68$ a.u. (for lower energies b_0 and R_{m0} are even larger), the incoming electron does not penetrate inside the cluster, which justifies the use of the spherical jellium model. Also, the perturbation being weak at large distances justifies the use of a first order many-body theory to compute the polarization potential. Consequently, the details of $U(R)$ for $R < R_{m0}$ are not needed for computation of the capture cross section.

According to the experiment [21], the measured electron energy distribution produced by the electron gun, $g(E - E_i)$, may be well represented by a Gaussian shape with a full width at half maximum of about 0.3 eV for $E \lesssim 1$ eV, and 0.4 eV for higher electron energies. Thus, in order to compare with the experiment we define the following quantity:

$$\tilde{\sigma}_{cap}(E_i) = \frac{\int_0^\infty \sigma_{cap}(E) \ g(E - E_i) dE}{\int_0^\infty g(E - E_i) dE}. \tag{32}$$

We show in Fig. 4, the capture cross sections calculated by using the above formula as a function of the electron impact energy for the three systems under study. The measured inelastic cross sections of [24] are also shown for comparison. For impact energies below 3 eV, essentially two processes participate in the inelastic signal: excitation via postcollisional fragmentation and electron capture, the latter being dominant at very low impact energy. The ionization process is absent since, for the clusters under study, the energy of the highest occupied molecular orbital is always higher than 3 eV.

First of all, the important difference existing between the TDLDA or the image charge results and those obtained by using the usual polarization potential $-q_1^2 \alpha_1(0)/2R^4$ indicates that it is necessary to go beyond the dipole approximation in order to describe the capture process correctly. As expected, this difference increases with increasing cluster size. Secondly, the difference between the TDLDA and the image charge results is not very important ($< 40\%$) and decreases slightly with increasing size of the cluster.

If the energy deposit in the clusters (which have been electronically excited during the collision) is larger than the lowest dissociation energy (~ 1 eV for sodium clusters), fragmentation can occur. Depending on the experimental time-of-flight window, the excited clusters (above the dissociation threshold) contribute or not to the experimental inelastic cross section. Since more vibrational degrees of freedom are involved for larger systems, at a given energy deposit, the fragmentation time increases with increasing number of atoms within the cluster. In the experiment of Ref. [24], the cluster velocities are of the order of 1000 m/s and the distance between the collision region and the beam de-

tector is 50 cm, which leads to a time-of-flight window $\tau_e \sim 5 \times 10^{-4}$ s. This means that excited clusters (with excitation energy E^*) having a fragmentation time $\tau_f(E^*) > \tau_e$ do not contribute to the inelastic cross section. Thus, according to the preceding arguments and assuming that the excitation spectrum does not change very much for the three clusters [this is true for photoexcitation ($L = 1$) [25]], the difference between the capture and the experimental inelastic cross sections must decrease with increasing cluster size. This behavior is illustrated in Fig. 4. Only for Na_{58} is a good agreement found between the TDLDA results and the experimental inelastic cross sections.

Very recently, the same authors [21] were able to measure only capture cross sections. Unfortunately, the experimental cross sections are not absolute and the experiment was not carried out with size selected clusters but rather with a cluster size distribution. Thus, a comparison with our predictions is not possible.

IV. CONCLUSION AND PERSPECTIVES

In summary, capture of low-energy electron by closed-shell sodium clusters has been studied by using the TDLDA within the spherical jellium model and the classical scattering theory of Langevin. The use of this model is completely justified since the capture process occurs well outside the cluster surface. Capture cross sections have been computed for Na_{20}, Na_{40}, and Na_{58} and compared with the predictions of the classical image charge model and recent experimental results by Kasperovich *et al.* [24]. It has been shown that in the range of impact energies considered in this work ($E < 3$ eV) the TDLDA capture cross sections are always larger than the classical ones obtained by using the macroscopic image charge model. As expected, the difference between the two predictions decreases with increasing cluster size. For Na_{58}, a good agreement is found between the TDLDA results and the experimental inelastic cross sections.

It is worth noticing that the present model does not include dynamical effects which seem to play some role in the capture process [4].

The same model can be applied to study electron attachment to C_{60} fullerenes, for which experimental data are available [26]. The results will be presented in a fothcoming publication. Also, related to the fragmentation of doubly charged simple metal clusters [27], fusion barriers may be evaluated by using the same procedure. We will address our next paper to this case.

[1] W.A. Heer, Rev. Mod. Phys. **65**, 611 (1993).

[2] M. Brack, Rev. Mod. Phys. **65**, 677 (1993).

[3] C. Bréchignac and J.P. Connerade, J. Phys. B **27**, 3795 (1994).

[4] S. Sentürk, J.P. Connerade, D.D. Burgess, and N.J. Mason, J.

Phys. B **33**, 2763 (2000), and references therein.

[5] B. Zarour, J. Hanssen, P.A. Hervieux, M.F. Politis, and F. Martín, J. Phys. B **33**, L1 (2000).

[6] J.P. Connerade, L.G. Gerchikov, A.N. Ipatov, and S. Sentürk, J. Phys. B **33**, 5109 (2000).

[7] W.D. Knight *et al.*, Phys. Rev. B **31**, 2539 (1985).

[8] E. Benichou *et al.*, Phys. Rev. A **59**, R1 (1999).

[9] M. Bernath, O. Dragún, M.R. Spinella, H. Massmann, and J.M. Pacheco, Phys. Rev. A **52**, 2173 (1995).

[10] V. Kasperovich, K. Wong, G. Tikhonov, and V.V. Kresin, Phys. Rev. Lett. **85**, 2729 (2000).

[11] J. D. Jackson, *Classical Electrodynamics*, 2nd ed. (John Wiley, New York, 1962).

[12] O. Gunnarsson and B.I. Lundqvist, Phys. Rev. B **13**, 4274 (1976).

[13] E. K. U. Gross, J. F. Dobson, and M. Petersilka, in *Density Functional Theory II*, Topics in Current Chemistry, edited by R. F. Nalewajski Vol. 181 (Springer-Verlag, Berlin, 1996), p. 81.

[14] G. D. Mahan and K. R. Subbaswamy, *Local Density Theory of Polarizability* (Plenum Press, New York, 1990).

[15] M.J. Stott, E. Zaremba, and D. Zobin, Can. J. Phys. **60**, 211 (1982).

[16] O.J. Kroneisen, H.J. Lüdde, and R.M. Dreizler, Phys. Lett. A **222**, 405 (1996).

[17] We have checked that the inclusion of the first two terms in the expression (26) does not modify the results presented in this work.

[18] P. Langevin, Ann. Chim. Phys. **5**, 245 (1905).

[19] E. W. McDaniel, *Atomic Collisions: Electron and Photon Projectiles* (Wiley, New York, 1989).

[20] L. D. Landau and E. M. Lifshitz, *Mechanics*, 3rd ed. (Pergamon, Oxford, 1976).

[21] V. Kasperovich, G. Tikhonov, K. Wong, and V.V. Kresin, Phys. Rev. A **62**, 063201 (2000).

[22] E. Vogt and G.H. Wannier, Phys. Rev. **95**, 1190 (1954).

[23] C.E. Klots, J. Chem. Phys. **100**, 1035 (1994).

[24] V. Kasperovich, G. Tikhonov, K. Wong, P. Brockhaus, and V.V. Kresin, Phys. Rev. A **60**, 3071 (1999).

[25] M. Madjet, C. Guet, and W.R. Johnson, Phys. Rev. A **51**, 1327 (1995).

[26] V. Kasperovich, G. Tikhonov, and V.V. Kresin, Chem. Phys. Lett. **337**, 55 (2001).

[27] U. Näher, S. Bjørnholm, S. Fauendorf, F. Garcias, and C. Guet, Phys. Rep. **285**, 245 (1997).